

THREE-DIMENSIONAL THERMAL CLOAK WITH HOMOGENEOUS AND NONSINGULAR CONDUCTIVE MATERIALS

Tiancheng Han* and Zhengmao Wu

School of Physical Science and Technology, Southwest University, Chongqing 400715, China

Abstract—Most three-dimensional omnidirectional cloaks proposed to date (using optics, electromagnetics, and acoustics) are not easily realized, as they possess inhomogeneous and singular parameters imposed by the transformation-optic method. In this study, we theoretically demonstrate that a thermodynamic spherical cloak with homogeneous and finite conductivity and employing only naturally available conductive materials may be achieved. More interestingly, the thermal localization inside the coating layer can be tuned by anisotropy, which may lead to nearly perfect functionality in an incomplete cloak. The practical realization of such a homogeneous thermal cloak by using two naturally occurring materials has been suggested, which provides an unprecedentedly plausible way to flexibly achieve a thermal cloak and manipulate heat flow. Numerical experiments validate the excellent performance of the proposed homogeneous cloak functions.

1. INTRODUCTION

In the past several years, there have been many significant achievements in invisibility cloaking due to the pioneering theoretical works of Pendry et al. [1] and Leonhardt [2]. Because ideal electromagnetic cloaks generally have extremely complex constitutive parameters (inhomogeneous, anisotropic, and even singular), reduced two-dimensional cloaks have been experimentally demonstrated in the microwave region [3, 4]. In addition, novel cloak for hiding multiple objects [5], open cloak [6], and nonsingular cloak [7] have been theoretically investigated. Further reducing the possibility of practical cloaks [3–7], a carpet cloak has been proposed using a quasi-conformal

Received 6 September 2013, Accepted 16 October 2013, Scheduled 29 October 2013

* Corresponding author: Tiancheng Han (tchan123@swu.edu.cn).

mapping method to hide an object placed on the ground [8]. Both two-dimensional (2D) [9–13] and three-dimensional (3D) [14, 15] carpet cloaks have also been experimentally demonstrated using gradient refractive index materials or calcite crystals. To decouple electric and magnetic effects, static magnetic [16, 17] and static electric cloaks [18] with anisotropic but homogeneous permeability and conductivity, respectively, have been experimentally realized recently.

In addition to the manipulation of electromagnetic waves [1–15] and static electrical/magnetic fields [16–18], the theoretical tool of coordinate transformation has been extended to acoustic waves [19, 20], matter waves [21], elastic waves [22], and heat flux [23–31]. However, analogous to electromagnetic cloaking [1, 3], conventional thermal cloaking is dependent on its own geometry, and such cloaks are usually made of materials that are inhomogeneous and singular [23–27]; in turn, the practical applications of the thermal cloak may be limited [28]. More recently, the experimental realization of a 2D thermal cloak that utilizes latex rubber and processed silicone has been reported [29], and general design roadmap for creating such advanced 2D thermal cloak has been investigated [30]. This success motivates us to explore a general design strategy for creating a realizable 3D thermal cloak by using only homogeneous, non-singular, and natural conduction materials.

The contribution of this study is threefold. First, based on rigorous theoretical analysis, we propose a novel 3D thermal cloak that is homogeneous, non-singular, and only dominated by anisotropy and is much more advanced than transformation-based cloaks [27, 28, 31]. Second, a 3D cloak is more practical for cloaking real objects than is a 2D cloak [29]; more importantly, the proposed 3D cloak can also be fabricated by a multilayer composition approach that exploits two naturally occurring materials throughout. Third, the proposed 3D cloak is independent of geometrical size because its thermal conductivity is not obtained from coordinate transformation [31], thus, leading to more flexible application. In addition, another advanced property of the proposed 3D cloak is that the thermal localization inside the coating layer can be tuned by anisotropy; as a result, most heat is confined in the vicinity of the outer boundary of the cloak. This unique functionality allows production of a partially constructed cloak with excellent performance by judicious selection of natural materials.

2. THEORETICAL ANALYSIS

Based on the invariance of the heat conduction equation under coordinate transformations, transformation thermodynamics has provided a new method to easily manipulate heat flux [23]. The

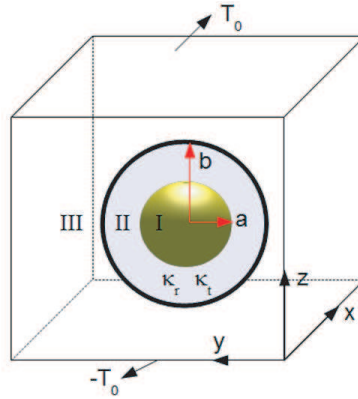


Figure 1. (Color online) Schematic of a homogeneous spherical thermal cloak.

ideal conductivity of the spherical cloak in Figure 1 is based on transformation thermodynamics and can be expressed as

$$\kappa_r = \frac{b}{b-a} \left(\frac{r-a}{r} \right)^2, \quad \kappa_t = \kappa_\theta = \kappa_\varphi = \frac{b}{b-a} \quad (1)$$

where κ_r and κ_t are radial and azimuthal thermal conductivities, respectively. a and b are inner radius and outer radius of thermal cloak, respectively. Clearly, the conductivity in Equation (1) is spatially variable and is singular at $r = a$ ($\kappa_r \rightarrow 0$), which is extremely difficult, if not impossible, to realize practically. Apart from the ideal case, construction of a homogeneous and nonsingular spherical cloak, in which κ_r and κ_t in the coating region are constant, is feasible in thermodynamics. Assuming κ_r and κ_t are constant in Figure 1, the thermal conduction equation $\nabla \cdot (\kappa \nabla T) = 0$ in spherical coordinates can be expanded as

$$\frac{\partial^2 T}{\partial r^2} + \frac{2}{r} \frac{\partial T}{\partial r} + \frac{\bar{\kappa}}{r^2 \sin \theta} \left[\frac{\partial}{\partial \theta} \left(\sin \theta \frac{\partial T}{\partial \theta} \right) + \frac{1}{\sin \theta} \frac{\partial^2 T}{\partial \varphi^2} \right] = 0 \quad (2)$$

where $\bar{\kappa} = 1$ for region I ($0 \leq r \leq a$) and III ($r > b$), and $\bar{\kappa} = \kappa_t / \kappa_r$ for region II ($a \leq r \leq b$). Considering the symmetry in the φ direction and antisymmetry in the z direction, the temperature potential of each of the three regions can be expressed as

$$T_1 = \sum_{m=1}^{\infty} A_{2m-1} r^{2m-1} P_{2m-1}(\cos \theta) \quad (3a)$$

$$T_2 = \sum_{m=1}^{\infty} \left[B_{2m-1} r^{l_m^+} + C_{2m-1} r^{l_m^-} \right] P_{2m-1}(\cos \theta) \quad (3b)$$

$$T_3 = \sum_{m=1}^{\infty} \left[D_{2m-1} r^{2m-1} + E_{2m-1} r^{-2m} \right] P_{2m-1}(\cos \theta) \quad (3c)$$

where $l_m^{\pm} = \frac{-1 \pm \sqrt{1+8\kappa_m(2m-1)}}{2}$, and $P_m(x)$ denotes the Legendre function of degree m .

The temperature potential and the normal component of the heat flux vector are continuous across the interfaces, meaning

$$\begin{cases} T_1|_{r=a} = T_2|_{r=a}, & \frac{\partial T_1}{\partial r}\bigg|_{r=a} = \kappa_r \frac{\partial T_2}{\partial r}\bigg|_{r=a} \\ T_2|_{r=b} = T_3|_{r=b}, & \kappa_r \frac{\partial T_2}{\partial r}\bigg|_{r=b} = \frac{\partial T_3}{\partial r}\bigg|_{r=b} \end{cases} \quad (4)$$

Assuming $\kappa_r l_1^+ = 1$ and $\kappa_r l_1^- = -1$ and combining the boundary conditions $T|_{z=\pm z_0} = \pm T_0$ and $\frac{\partial T}{\partial x}\big|_{x=\pm x_0} = 0$, $\frac{\partial T}{\partial y}\big|_{y=\pm y_0} = 0$, we obtain

$$T_1 = \frac{T_0}{z_0} \left(\frac{a}{b}\right)^{l_1^+-1} r \cos \theta, \quad T_2 = \frac{T_0}{z_0} \left(\frac{r}{b}\right)^{l_1^+-1} r \cos \theta, \quad T_3 = \frac{T_0}{z_0} r \cos \theta \quad (5)$$

Clearly, if $l_1^+ = 1$, i.e., $\kappa_r = \kappa_t$, we can obtain $T_1 = T_2 = T_3$, which denotes free space. If $l_1^+ \gg 1$, we can obtain $T_1 \rightarrow 0$, which means that a spherical cloak is formed. We conclude that the necessary and sufficient conditions for achieving a nearly perfect spherical cloak include $\kappa_r l_1^+ = 1$, $\kappa_r l_1^- = -1$, and $l_1^+ \gg 1$. If $l_1^+ \gg 1$, we can obtain $\kappa_r \ll \kappa_t$. Obviously, ideal κ_r and κ_t values are not available that rigorously satisfy the conditions $\kappa_r l_1^+ = 1$, $\kappa_r l_1^- = -1$ and $l_1^+ \gg 1$. However, fairly accurate approximate κ_r and κ_t values can be obtained with the relationship

$$\kappa_t = \frac{\sqrt{1 - \kappa_r^2}}{2\kappa_r} \quad (6)$$

where $0 < \kappa_r < 1$ and $\kappa_t > 1$.

To further validate the proposed methodology, we can substitute Equation (6) into Equation (3) to determine the coefficients A and E . For an ideal cloak, A and E should be zero, which means that the external field is repelled to touch the cloaking region, and the external field outside the cloak is not disturbed. When $\kappa_r = 0.1$, rigorous calculations demonstrate that A and E are less than 3% and 0.2% of the external field, respectively. A nearly perfect homogeneous 3D thermal cloak that is dominated by only anisotropy has clearly been achieved.

3. SIMULATIONS AND DISCUSSION

To validate the proposed homogeneous spherical cloak, full-wave simulations are carried out based on the finite element method (FEM). Figure 2 shows the temperature profiles of a spherical thermal cloak with inner and outer radii of $a = 0.2\text{m}$ and $b = 0.4\text{m}$, respectively. Figure 2(a) corresponds to the ideal spherical cloak with inhomogeneous parameters as described in Equation (1), and Figures 2(b)–(d) correspond to proposed homogeneous cloaks with different constant conductivities. In all cases, the heat fluxes travel around the inner domain and eventually return to their original pathway. Therefore, the object inside the inner domain is protected

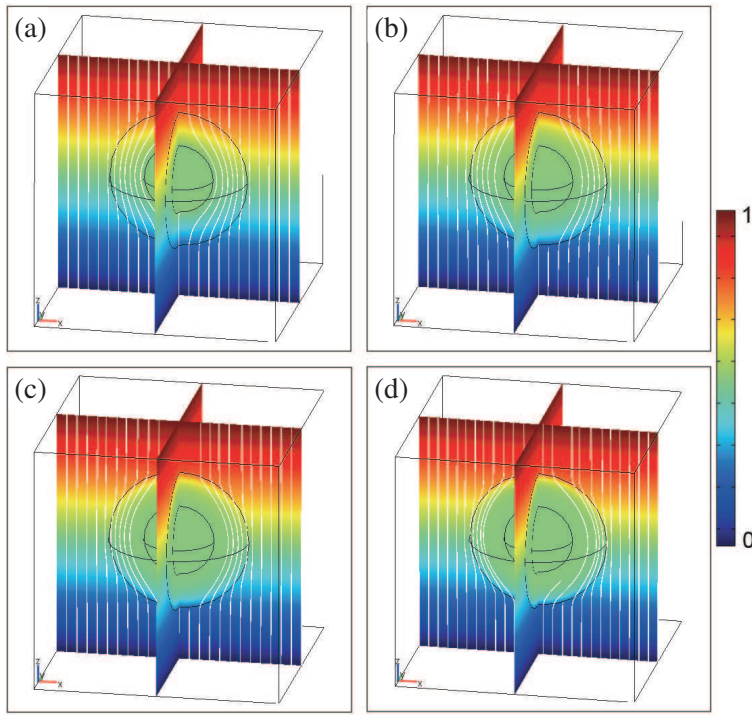


Figure 2. (Color online) Temperature profiles for spherical thermal cloaks with $a = 0.2\text{m}$ and $b = 0.4\text{m}$. (a) Ideal cloak with inhomogeneous and anisotropic conductivity as described in Equation (1). (b) $\kappa_r = 0.2$ and $\kappa_t = 2.5$. (c) $\kappa_r = 0.15$ and $\kappa_t = 3.3$. (d) $\kappa_r = 0.1$ and $\kappa_t = 5$. Streamlines of thermal flux are also represented with white color in the panel.

from the invasion of external heat flux. Clearly, we have achieved an advanced spherical cloak with extremely simple parameters (finite constant conductivity) that has performance as perfect as the ideal case. More interestingly, the isothermal lines are more concentrated near the outer boundary as anisotropy increases, which accords well with the prediction of the theoretical equation $T_2/T_3 = (r/b)^{l_1^+ - 1}$. This property may lead to an incomplete cloak with excellent performance.

This proposed cloak with homogeneous conductivity could be easily realized by alternating layered isotropic media, and only two types of isotropic materials (media A and B) are needed throughout, as shown in Figure 3(a). The conductivities of media A and B

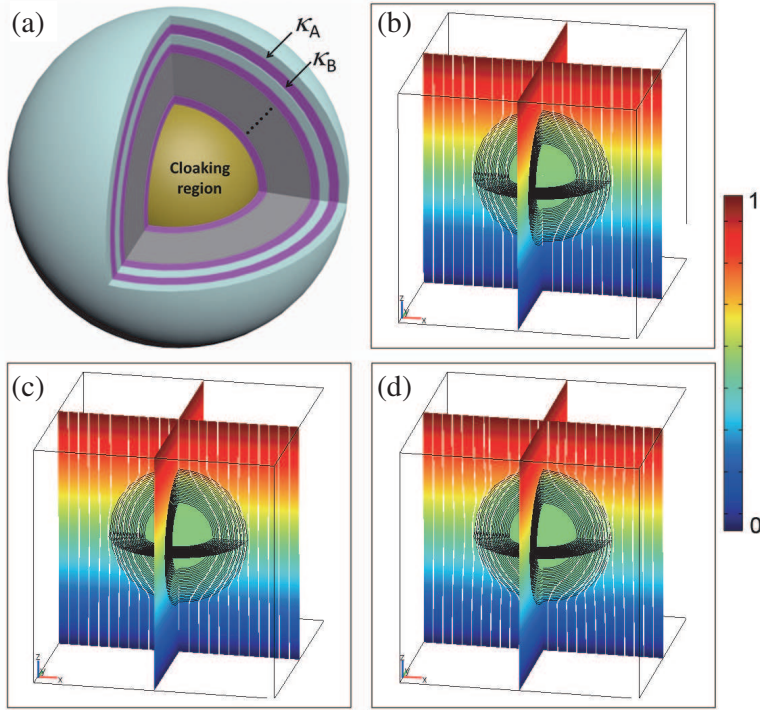


Figure 3. (Color online) Temperature profiles for multilayered spherical thermal cloaks with homogeneous and isotropic conductivity. (a) The scheme for realization of the spherical cloaks in Figure 2 with multilayered structures. (b) $\kappa_A = 2.8$ and $\kappa_B = 0.06$. (c) $\kappa_A = 3.7$ and $\kappa_B = 0.04$. (d) $\kappa_A = 5.6$ and $\kappa_B = 0.03$. Streamlines of thermal flux are also represented with white color in the panel.

can be obtained by $\kappa_{A,B} = \kappa_t \pm \sqrt{\kappa_t^2 - \kappa_r \kappa_t}$. In the following simulations, the cloaking shell is equally discretized into 10 layers, and each layer is composed with medium A and B. Figures 3(b)–(d) show the multilayered compositions for realization of the cloaks in Figures 2(b)–(d). The multilayered cloak with homogeneous, isotropic, and nonsingular conductivities clearly functions as perfectly as the ideal case. The anisotropy in Figure 2 has been removed by replacing the anisotropic material with two naturally occurring materials, such as thermal epoxy (with conductivity $2 \sim 6$) and wood (with conductivity $0.04 \sim 0.4$), as shown in Figure 3(a).

To quantitatively examine the performance of the proposed homogeneous and isotropic spherical cloak in Figure 3, Figure 4 shows the temperature distribution along the z -axis of a cloak with different constant conductivities. As observed in Figure 4, the temperature is always kept constant in the cloaking region ($r \leq 0.2$ m) but variant in the coating region ($0.2 \text{ m} \leq r \leq 0.4$ m) with different conductivities. This result once again validates the excellent performance of the proposed cloak. More interestingly, the temperature distribution in the coating is more concentrated near its outer boundary as a result of the increased anisotropy ($\bar{\kappa}$), which means that the cloaking region can be enlarged while the outer boundary is kept invariant. Acceptable invisibility performance with minimum anisotropy is desired for practical realization of the cloak. If the anisotropy is too large, practical realization becomes difficult; therefore, a balance between the two quantities is required.

The proposed homogeneous 3D cloak has good performance not

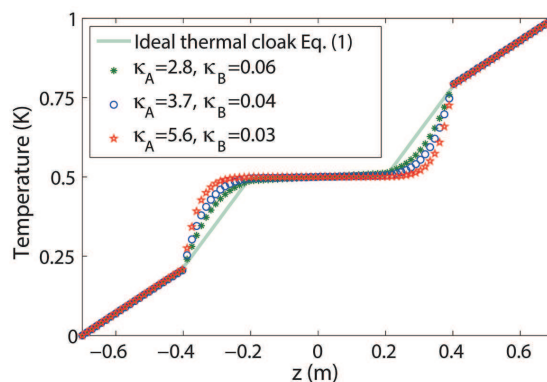


Figure 4. (Color online) The temperature distribution along the z -axis for the multilayered spherical cloak with $a = 0.2$ m and $b = 0.4$ m.

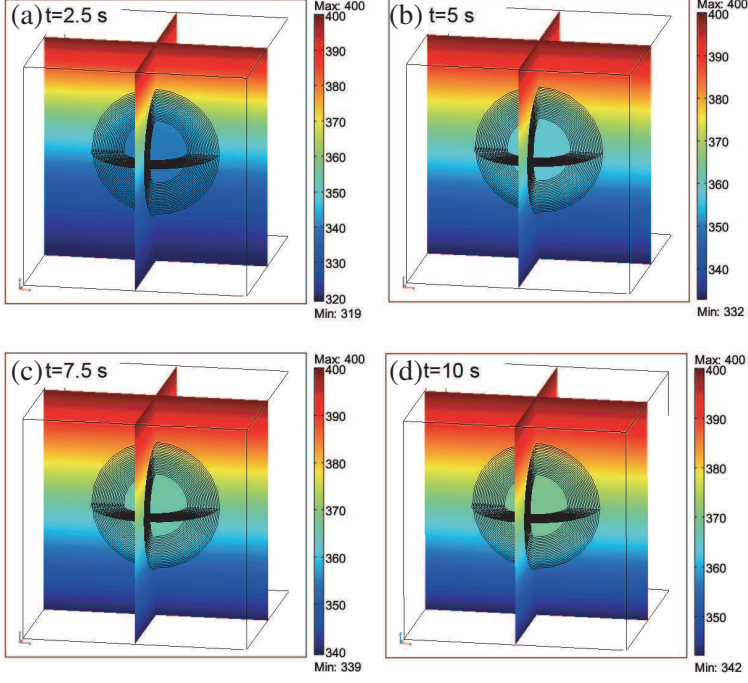


Figure 5. (Color online) The time dependent diffusion of heat from the top of the cloak in Figure 3(b). Snapshots of temperature distribution at (a) $t = 2.5$ s, (b) $t = 5$ s, (c) $t = 7.5$ s, (d) $t = 10$ s.

only in the steady state but also the time dependent case. Figure 5 shows the real-time temperature distribution of the cloak in Figure 3(b) when we apply a constant temperature (400 K) on the top and a convective flux boundary condition on the bottom. The surrounding is set at room temperature (300 K). The central cloaking region displays specific protection against heat, as the isothermal surface goes around the central region without distortion, and heat flux never enters the central region to touch the cloaking object. The temperature of the cloaking region allowed to vary with time is always constant because the inner boundary of the cloak is continuous, which causes the temperature of the central region to be equal to the temperature at the inner boundary ($r = a$). When $t > 10$ s, the temperature distribution is no longer invariant, which is a steady state analogous to Figure 3(b).

4. CONCLUSION

To conclude, we have proposed an advanced methodology for creating a 3D thermal cloak with finite constant conductivity (without inhomogeneity and singularity) that drastically facilitates feasible realization and fabrication. The proposed cloak is independent of its geometrical size and only dominated by anisotropy, which could be easily replaced by periodically alternating isotropic conductivities. Most interestingly, the thermal localization inside the coating layer can be tuned by anisotropy, which may lead to excellent performance in an incomplete cloak. Theoretical analysis and full-wave simulations validate the advanced thermal cloak composed of simple materials. The most recently reported spherical thermal cloak is still inhomogeneous and singular [31], requiring $2N$ different types of conductivities, where N is the total number of discretization layers.

ACKNOWLEDGMENT

Tiancheng Han acknowledges the support from the National Natural Science Foundation of China under Grant No. 11304253 and the support from the Southwest University (SWU112035).

REFERENCES

1. Pendry, J. B., D. Schurig, and D. R. Smith, "Controlling electromagnetic fields," *Science*, Vol. 312, 1780–1782, 2006.
2. Leonhardt, U., "Optical conformal mapping," *Science*, Vol. 312, 1777–1780, 2006.
3. Schurig, D., J. J. Mock, B. J. Justice, S. A. Cummer, J. B. Pendry, A. F. Starr, and D. R. Smith, "Metamaterial electromagnetic cloak at microwave frequencies," *Science*, Vol. 314, 977–980, 2006.
4. Kanté, B., D. Germain, and A. Lustrac, "Experimental demonstration of a nonmagnetic metamaterial cloak at microwave frequencies," *Phys. Rev. B*, Vol. 80, 201104, 2009.
5. Han, T. C., X. H. Tang, and F. Xiao, "The petal-shaped cloak," *Journal of Electromagnetic Waves and Applications*, Vol. 23, Nos. 14–15, 2055–2062, 2009.
6. Han, T. C., C.-W. Qiu, and X. H. Tang, "Creating rigorous open cloaks," *Journal of Electromagnetic Waves and Applications*, Vol. 24, No. 13, 1839–1847, 2010.
7. Cummer, S. A., R. P. Liu, and T. J. Cui, "A rigorous and

- nonsingular two dimensional cloaking coordinate transformation,” *J. of Appl. Phys.*, Vol. 105, 056102, 2009.
8. Li, J. and J. B. Pendry, “Hiding under the carpet: A new strategy for cloaking,” *Phys. Rev. Lett.*, Vol. 101, 203901, 2008.
 9. Liu, R., C. Ji, J. J. Mock, J. Y. Chin, T. J. Cui, and D. R. Smith, “Broadband ground-plane cloak,” *Science*, Vol. 323, 366–369, 2009.
 10. Valentine, J., J. Li, T. Zentgraf, G. Bartal, and X. Zhang, “An optical cloak made of dielectrics,” *Nat. Mater.*, Vol. 8, 568–571, 2009.
 11. Gabrielli, L. H., J. Cardenas, C. B. Poitras, and M. Lipson, “Silicon nanostructure cloak operating at optical frequencies,” *Nat. Photon.*, Vol. 3, 461–463, 2009.
 12. Zhang, B., Y. Luo, X. Liu, and G. Barbastathis, “Macroscopic invisibility cloak for visible light,” *Phys. Rev. Lett.*, Vol. 106, 033901, 2011.
 13. Chen, X., Y. Luo, J. Zhang, K. Jiang, J. B. Pendry, and S. Zhang, “Macroscopic invisibility cloaking of visible light,” *Nat. Commun.*, Vol. 2, 176, 2011.
 14. Ma, H. F. and T. J. Cui, “Three-dimensional broadband ground-plane cloak made of metamaterials,” *Nat. Commun.*, Vol. 1, 21, 2010.
 15. Ergin, T., N. Stenger, P. Brenner, J. B. Pendry, and M. Wegener, “Three-dimensional invisibility cloak at optical wavelengths,” *Science*, Vol. 328, 337–339, 2010.
 16. Sanchez, A., C. Navau, J. Prat-Camps, and D. X. Chen, “Antimagnets: Controlling magnetic fields with superconductor-metamaterial hybrids,” *New J. Phys.*, Vol. 13, 093034, 2011.
 17. Gömöry, F., M. Solovyov, J. Šouc, C. Navau, J. Part-Camps, and A. Sanchez, “Experimental realization of a magnetic cloak,” *Science*, Vol. 335, 1466–1468, 2012.
 18. Jiang, W. X., C. Y. Luo, Z. L. Mei, and T. J. Cui, “An ultrathin but nearly perfect direct current electric cloak,” *Appl. Phys. Lett.*, Vol. 102, 014102, 2013.
 19. Chen, H. and C. T. Chan, “Acoustic cloaking in three dimensions using acoustic metamaterials,” *Appl. Phys. Lett.*, Vol. 91, 183518, 2007.
 20. Zhang, S., C. Xia, and N. Fang, “Broadband acoustic cloak for ultrasound waves,” *Phys. Rev. Lett.*, Vol. 106, 24301, 2011.
 21. Zhang, S., D. A. Genov, C. Sun, and X. Zhang, “Cloaking of matter waves,” *Phys. Rev. Lett.*, Vol. 100, 123002, 2008.

22. Brun, M., S. Guenneau, and A. B. Movchan, "Achieving control of in-plane elastic waves," *Appl. Phys. Lett.*, Vol. 94, 061903, 2009.
23. Milton, G. W., M. Briane, and J. R. Willis, "On cloaking for elasticity and physical equations with a transformation invariant form," *New J. Phys.*, Vol. 8, 248, 2006.
24. Fan, C., Y. Gao, and J. Huang, "Shaped graded materials with an apparent negative thermal conductivity," *Appl. Phys. Lett.*, Vol. 92, 251907, 2008.
25. Chen, T., C. N. Weng, and J. S. Chen, "Cloak for curvilinearly anisotropic media in conduction," *Appl. Phys. Lett.*, Vol. 93, 114103, 2008.
26. Li, J., Y. Gao, and J. Huang, "A bifunctional cloak using transformation media," *J. Appl. Phys.*, Vol. 108, 074504, 2010.
27. Guenneau, S., C. Amra, and D. Veynante, "Transformation thermodynamics: Cloaking and concentrating heat flux," *Opt. Express*, Vol. 20, 8207–8218, 2012.
28. Schittny, R., M. Kadic, S. Guenneau, and M. Wegener, "Experiments on transformation thermodynamics: Molding the flow of heat," *Phys. Rev. Lett.*, Vol. 110, 195901, 2013.
29. Narayana, S. and Y. Sato, "Heat flux manipulation with engineered thermal materials," *Phys. Rev. Lett.*, Vol. 108, 214303, 2012.
30. Han, T. C., T. Yuan, B. W. Li, and C. W. Qiu, "Homogeneous thermal cloak with constant conductivity and tunable heat localization," *Scientific Reports*, Vol. 3, 1593, 2013.
31. Guenneau, S. and T. M. Puvirajesinghe, "Fick's second law transformed: One path to cloaking in mass diffusion," *J. R. Soc. Interface*, Vol. 10, 20130106, 2013.